



Please cite the Published Version

Sulaiman, Mira Mohideen, Fatalla, Abdalbseet Ahmad  and Haider, Julfikar  (2024) The Impact of Incorporating Grapefruit Seed Skin Particles into 3D-Printed Acrylic Resin on Mechanical Properties. *Prosthesis*, 6 (6). pp. 1420-1436.

DOI: <https://doi.org/10.3390/prosthesis6060103>

Publisher: MDPI

Version: Published Version

Downloaded from: <https://e-space.mmu.ac.uk/637465/>

Usage rights:  [Creative Commons: Attribution 4.0](https://creativecommons.org/licenses/by/4.0/)

Additional Information: This is an open access article which first appeared in *Prosthesis*, published by MDPI

Data Access Statement: The data presented in this study are available on request from the corresponding author.

Enquiries:

If you have questions about this document, contact openresearch@mmu.ac.uk. Please include the URL of the record in e-space. If you believe that your, or a third party's rights have been compromised through this document please see our Take Down policy (available from <https://www.mmu.ac.uk/library/using-the-library/policies-and-guidelines>)

Article

The Impact of Incorporating Grapefruit Seed Skin Particles into 3D-Printed Acrylic Resin on Mechanical Properties

Mira Mohideen Sulaiman ¹, Abdalbseet Ahmad Fatalla ^{1,*}  and Julfikar Haider ^{2,*} 

¹ Department of Prosthodontics, College of Dentistry, University of Baghdad, Baghdad 1417, Iraq; mera.muhi2201@codental.uobaghdad.edu.iq

² Department of Engineering, Manchester Metropolitan University, Manchester M12 5GN, UK

* Correspondence: abdalbasit@codental.uobaghdad.edu.iq (A.A.F.); j.haider@mmu.ac.uk (J.H.)

Abstract: Background: Grapefruit seed skin particles (GSSPs) have antifungal properties due to the presence of flavonoids. Therefore, it has the potential to display antifungal characteristics when added to acrylic resin, but it could affect the mechanical properties of the resin. This study investigated the effects of adding GSSPs on the mechanical characteristics of 3D-printed denture base resins. Purpose: The aim of the present study was to determine the effects of the addition of GSSPs to 3D-printed acrylic at different concentrations on the degree of conversion (DC), surface hardness, flexural strength, and tensile strength. Methods: In this study, 90 samples were printed with acrylic resin via a Digital Light Processing (DLP) printer. Thirty square samples were used for the surface hardness test. Thirty rectangular samples were used for the flexural strength test, and thirty dumbbell-shaped samples were used for the tensile strength test. These materials were prepared by adding different concentrations of GSSPs (0.0 wt.%, 5.0 wt.%, and 7.0 wt.%), which were determined by a pilot study to be the most effective in 3D denture base resins. The Durometer Shore Hardness Scale (DSHS) was used to measure the surface hardness, and a universal testing machine was employed to gauge the flexural strength and tensile strength. Field emission scanning electron microscopy (FE-SEM) was employed for particle size analysis and fracture behavior determination. Results: Compared with those of the control group, the degree of conversion (DC), surface hardness, flexural strength, and tensile strength of the treated groups significantly improved after the addition of 5.0 wt.% and 7.0 wt.% GSSPs. The FE-SEM images revealed a decrease in porosity as the concentration of GSSPs increased with a brittle fracture behavior. Conclusions: The addition of GSSPs to 3D-printed acrylic is recommended because of their significant positive impacts on the mechanical properties of 3D-printed denture base resin.



Citation: Sulaiman, M.M.; Fatalla, A.A.; Haider, J. The Impact of Incorporating Grapefruit Seed Skin Particles into 3D-Printed Acrylic Resin on Mechanical Properties. *Prosthesis* **2024**, *6*, 1420–1436. <https://doi.org/10.3390/prosthesis6060103>

Academic Editors: Fernando Zarone, Roberto Sorrentino and Gennaro Ruggiero

Received: 28 September 2024

Revised: 15 November 2024

Accepted: 20 November 2024

Published: 29 November 2024



Copyright: © 2024 by the authors. Licensee MDPI, Basel, Switzerland. This article is an open access article distributed under the terms and conditions of the Creative Commons Attribution (CC BY) license (<https://creativecommons.org/licenses/by/4.0/>).

Keywords: 3D printing; acrylic resin; denture; grapefruit seed skin particles; hardness; flexural strength; tensile strength

1. Introduction

Partial and complete edentulism has been a major health problem in countries because of the aging population and poor oral hygiene. Installing dentures is considered to be the solution for this problem [1]. To obtain these dentures, patients must make at least five visits to the clinic, and most of these clinical and laboratory procedures are performed manually. Therefore, it is difficult to ensure quality and dimensional consistency and to reuse and maintain physical models [2].

With the development of technology, the use of computerized techniques in dental prosthetic fabrication has come into play. Three-dimensional (3D) printers are among these technologies and are also referred to as additive manufacturing (AM) technology [3], which was developed in the 1980s [4]. AM technology involves the layer-by-layer construction of an object [5]. The development of AM technology has permitted its use in prosthodontic applications [6]. Seven categories of AM have been determined by the American Section

of the International Association for Testing Material F42 [5,6]. Material jetting (MJ) and stereolithography (SLA) are the most widely used additive manufacturing technologies in dentistry. The SLA consists of a building platform immersed in liquid resin. This resin is polymerized by an ultraviolet laser. The cross-section for each layer in the object is traced by the laser. The building platform moves a distance equal to the polymerized layer thickness to allow the uncured resin to be placed over the previous layer. This procedure is repeated multiple times until the complete object is constructed [3,6].

The most common problem in patients wearing dentures is denture stomatitis, which manifests as the inflammation of the tissue under the complete denture base [7]. The treatment of denture stomatitis could involve enhancing dentures and following the guidelines for oral hygiene [8]. Numerous studies have discussed the addition of antifungal material to denture bases, but this addition must be performed with caution to ensure biological compatibility, ease of manipulation, and cost effectiveness [9]. Some of the natural materials that have been added are chitosan [10], henna [8], and lemongrass essential oils [11], whereas other methods based on the immersion of dentures in cleansing solutions such as tea tree oil have also been reported in the literature [12]. Grapefruit seed extract, which is rich in flavonoids, has been shown to have inhibitory effects on *Candida albicans* species [13,14]; therefore, it is reported to have powerful antifungal properties [14]. However, there are no studies on the effects of the addition of grapefruit skin seed microparticles to 3D-printed acrylic on the resulting mechanical properties.

This study aimed to determine the surface hardness, flexural strength, and tensile strength of 3D-printed acrylic after the addition of GSSPs at concentrations of 0.0, 5.0, and 7.0 wt.%. In addition, calculating the degree of conversion (DC) is necessary to determine the amount of uncured resin (unpolymerized monomer) that causes irritation to the oral mucosa and affects the mechanical and physical properties of the material [15]. The null hypotheses assumed that there would be no effect on the mechanical properties of 3D-printed denture base resin after the addition of grapefruit seed skin microparticles.

2. Materials and Methods

2.1. Powder Preparation

Locally grown fresh grapefruit was purchased from a supermarket in Baghdad. With a sharp blade, the fruits were cut into small pieces, the seeds were collected by hand, and the same blade was used to peel the seeds. The peels were washed with tap water and then dried in an oven at 40 °C for 24 h [16]. Next, a planetary ball mill (NQM-0,4 model planetary ball mill, MTI Corporation, Richmond, CA, USA) was used to create micro-sized particles [17].

2.2. Preparation of the Samples

The 3D-printed material used in this study was a light-cure denture base resin (Optiprint Laviva) with a light-pink color manufactured by Dentona, Dortmund, Germany. The 3D denture base resin was poured into a dark bottle and heated to 60 °C for 30 min (78–1 magnetic heating stirrer, India) to decrease its viscosity. The powder was then added after being weighed with a 3-digit electrical scale (DM3, UK) as described in Table 1, and the mixture was stirred at room temperature at 2400 rpm for 8 h with the magnetic stirrer to obtain a homogeneous mixture. This mixture was then ready for 3D printing [18]. The samples for each test were divided into three groups ($n = 10$): control, 5.0 wt.% GSSPs, and 7.0 wt.% GSSPs, which was determined by a pilot study as the most effective reinforcement of 3D denture base resin.

Table 1. Weight percentage (wt.%) of grapefruit seed skin particles (GSSPs) added to 3D-printed liquid resin.

Groups	3D-Printed Liquid Resin (g)	Grapefruit Seed Skin Particles (g)
0.0 wt.% (Control)	100.0	0.0
5.0 wt.%	95.0	5.0
7.0 wt.%	93.0	7.0

The printing process began by transmitting the stereolithography (STL) file (the sample's software design) from the microform computer software program to the 3D printer (DLP, Microlay Versus 385, European). The software settings for the resin were adjusted according to the manufacturer's instructions, with a layer thickness of 50 μm and a 45-degree printing orientation. This printing orientation was chosen according to Mudhaffer et al., who reported that the 45° orientation produced mechanical properties greater than that at 0° [19]. A total of 90 samples were printed for use in this study. In accordance with ISO specifications (20795-1:2013), 30 square samples (12 mm \times 12 mm \times 3 mm \pm 0.2 mm in length, width, and thickness) were printed for surface hardness testing, and 30 rectangular samples (64 mm \times 10 mm \times 3.3 mm \pm 0.2 mm in length, width, and thickness) were printed for flexural strength testing. For tensile testing, the samples were printed according to the American Society for Testing Materials (ASTM) D638 specifications in a dumbbell shape with a length of 75 \pm 0.2 mm, an average center section width of 12 \pm 0.2 mm, and a thickness of 2.5 \pm 0.2 mm. Each batch contained 5 samples and took 2 h 17 min for surface-hardness samples, 2 h 23 min for flexural samples, and 2 h 31 min for tensile samples.

After printing, the samples were placed in 99.9% isopropyl alcohol (Alpha Chemika, Mumbai, India) to separate any uncured resin. The samples were then immersed in glycerol (Thomas Baker, Mumbai, India) before being exposed to an ultraviolet (UV) light curing machine (Creality UW-01, UK) for 20 min according to the manufacturer's instructions to complete the polymerization process. The base and support structures were removed via a low-speed handpiece (Saeyang Marathon Multi 600 Brushless Micromotor Handpiece 50,000 rpm Micro Motor, Republic of Korea), and silicon carbide papers (800, 1500, and 2000 grit) were used to polish the samples. The step-by-step sample preparation procedure involved the use of a digital Vernier scale (Kirti NDT, Dombivli East, India) to measure the dimensions of the samples. Finally, the samples were immersed in distilled water for 48 h before they were subjected to the testing procedure [20]. Figure 1 presents the step-by-step procedure for sample preparation.

2.3. Testing Procedures

A digital Shore D durometer hardness tester (TH 210, Beijing Time High Technology Ltd., Beijing, China) was used to perform the test. Five readings were taken for each sample, according to ISO 20795-1:2013, and the mean value was then calculated.

Three-point bending was applied via a universal testing machine (Instron, model WDW-20) equipped with a 20 kN load cell. According to ISO 20795-1:2013, this machine has a central loading plunger and two supports with a 50 mm distance between them. These have cylindrical, polished surfaces with a 3.2 mm radius, and they were made parallel to one another and perpendicular to the centerline. The central loading plunger is placed in the middle of the two supports. This test was performed at a constant loading rate of 5 mm/min. A steady force (from zero) was applied to the sample through the plunger until it fractured. The fracture load was recorded in Newtons (N), and the following equation was employed to determine the flexural strength.

$$\sigma_f = \frac{3FL}{2bh^2} \quad (1)$$

where σ_f is the flexural strength (MPa), F is the highest load before fracture (N), L is the length between two supports (mm), b is the width of the printed sample (mm), and h is the height of the printed sample (mm).

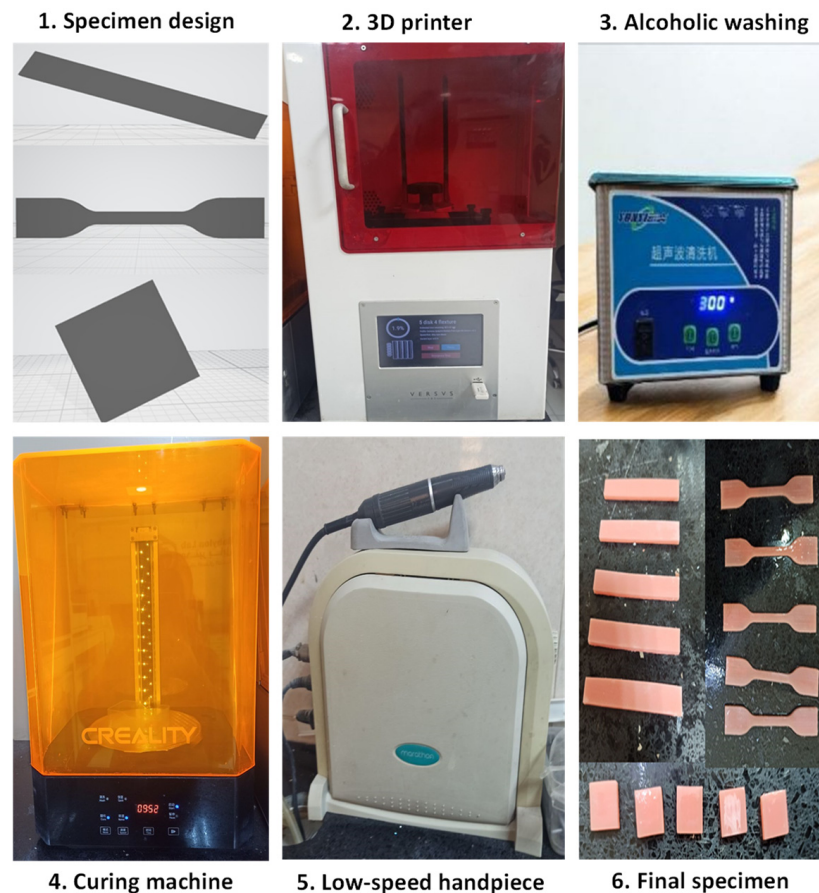


Figure 1. Fabrication steps of 3D-printed resin reinforced with grapefruit seed skin particles.

The tensile strength test was performed in the same universal testing machine (UTM) by applying a tensile force on the sample with a cross head speed of 5 mm/min according to the specification of American Society for Testing Materials (ASTM) D638 by clamping the ends of the dumbbell-shaped sample to two jigs separated by a certain distance. As the two jigs separated, the sample was stretched until fracture. The following equation is used for calculating the tensile strength:

$$\sigma_t = \frac{F_m}{A} \quad (2)$$

where σ_t is the tensile strength (MPa), F_m is the maximum force (N), and A is the cross-sectional area of the sample (mm^2).

One gram of GSSPs was taken to determine the size and shape of the particles by a scanning electron microscopy (SEM) (Philips Quanta250 electron) in secondary electron mode according to the following operating parameters (HV = 20.000 kV, WD = 4.1970 mm), and 2 g from the same powder was used to analyze the size and distribution with principles based on Dynamic Light Scattering (Brookhaven Instruments Corporation, 90 plus particle sizing software Ver. 5.34, Nashua, NH, USA). The same SEM was used to scan the surface of flexural strength samples before fracture after coating it with a thin layer of gold (HV = 20.000 kV, WD = 26.860 to 27 mm).

FE-SEM (TESCAN, Brno, Czech Republic) was used to investigate the fracture sites of the control and GSSPs-embedded resin samples at different concentrations (5.0 wt.%, 7.0 wt.%) during flexural testing. The fractured sites were coated with a thin layer of gold before scanning via the FE-SEM according to the following operating parameters (detector = Everhart–Thornley detector, ETD, HV = 30.000 kV, WD: 8.2 to 8.5 mm) to evaluate the distribution of the GSSPs and failure modes and mechanisms.

The FTIR spectra of the samples were recorded for a scan range between 400 and 4000 cm^{-1} with an FTIR spectrometer (IRAffinity-1 laser product, SHIMADZU, Kyoto, Japan) at a temperature of 22 ± 1 °C. To determine the degree of conversion, FTIR spectra for the liquid resin were obtained to provide a reference record and for the solid samples ($n = 3$) after complete polymerization of the square-shaped samples (12 mm \times 12 mm \times 3 mm \pm 0.2 mm). Equation (3) was used to determine the DC of the sample by calculating the ratio of the aliphatic (C=C) peak height at 1635 cm^{-1} to the aromatic (C=O) peak heights at 1716, 1728, and 1720 cm^{-1} for the control, 5.0 wt.%, and 7.0 wt.% groups, respectively.

$$DC = \left(1 - \frac{\left(\frac{A_{C=C}}{A_{C=O}} \right)_{polymer}}{\left(\frac{A_{C=C}}{A_{C=O}} \right)_{monomer}} \right) \times 100 \quad (3)$$

2.4. Statistical Analysis

Prism 9 (GraphPad Software, La Jolla, CA, USA) was used to analyze the data statistically. The Shapiro-Wilk test was used to determine the normality of the data, whereas the Brown–Forsythe test was performed to verify the homogeneity of the data. ANOVA was performed to study the interaction between the groups, and the Games–Howell multiple comparisons test was carried out to identify any discrepancies with a confidence interval value of 95% and an alpha value of 0.05.

3. Results

3.1. SEM and Particle Size Analysis

Figure 2 shows SEM images of the GSSPs, which were randomly shaped and tended to congregate because of their high contact areas. A particle size analysis revealed that the average particle diameter was 6327.0 nm.

3.2. Hardness, Flexural Strength, and Tensile Strength

The descriptive statistics for the surface hardness test revealed an increase in the mean values as the concentration of GSSPs increased. The lowest mean value was 90.11 for the control group, and the highest mean value was 93.41 for the 7.0 wt.% GSSP concentration group. Figure 3 shows significant differences between the reinforced groups and the control group and within the reinforced groups ($p < 0.0001$).

The descriptive statistics for the flexural strength test revealed an increase in the mean values as the concentration of GSSPs increased; the lowest mean value was 66.36 MPa for the control group, and the highest mean value was 77.98 MPa for the 7.0 wt.% concentration group. Figure 3 showed a significant difference for both the reinforced groups within themselves and the reinforced groups and the control group ($p < 0.0001$).

The descriptive statistics for the tensile strength test revealed an increase in the mean values as the concentration of GSSPs increased; the lowest mean value was 15.1 MPa for the control group, and the highest mean value was 21.04 MPa for the 7.0 wt.% concentration group. Figure 3 shows significant differences between the reinforced groups and the control group and within the reinforced groups ($p < 0.0001$).

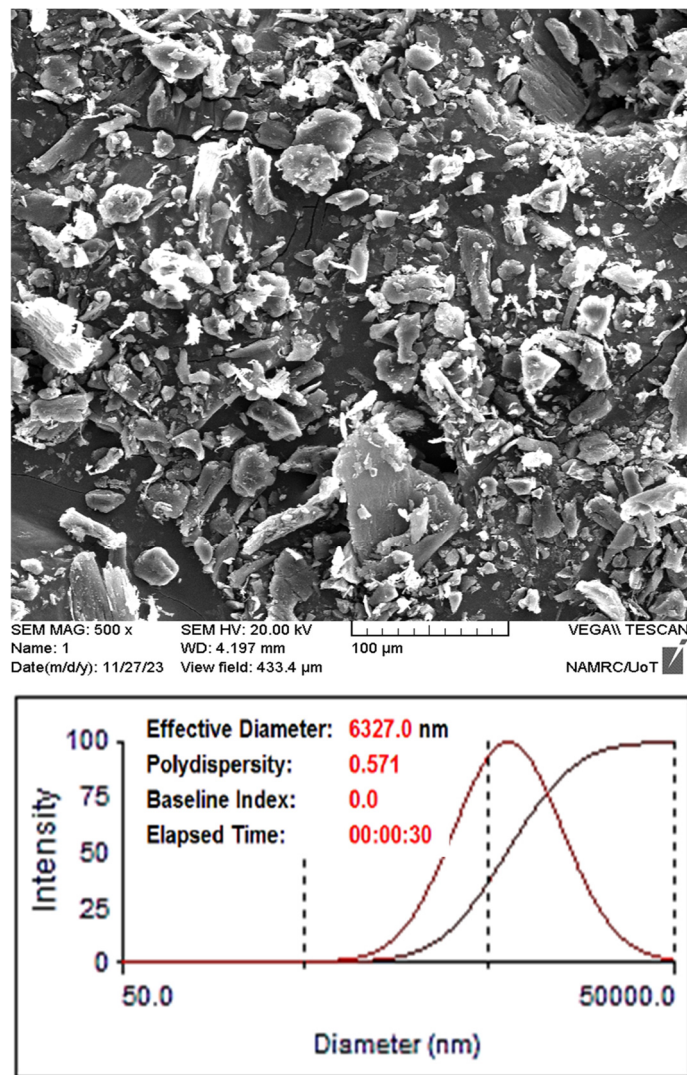


Figure 2. Scanning electron microscopy and particle size analysis of grapefruit seed skin microparticles.

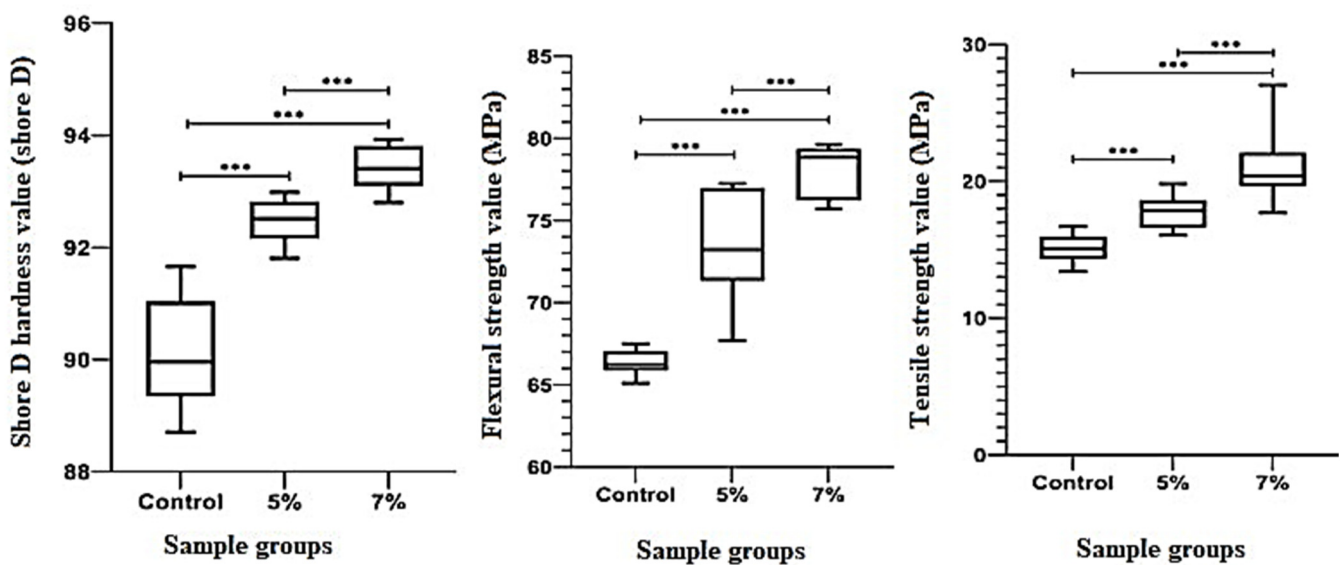


Figure 3. Boxplots for the surface hardness, flexural strength, and tensile strength results with multiple comparisons labeled with ***. A p value < 0.001 indicated high statistical significance (***).

3.3. Fracture Modes and Mechanisms

FE-SEM images of the fracture sites in 3D-printed pure acrylic and composites reinforced with 5.0 wt.% and 7.0 wt.% GSSPs before and after flexural tests are shown in Figures 4 and 5, respectively. In these images, the microstructure of the granules was noticeable, and an even distribution of particles within the resin matrix was observed that achieved homogenous material in addition to good interfacial adhesion of the matrix and GSSPs, which contributed to the enhancement of the mechanical properties. They revealed larger voids in the control group, whereas the 5.0 wt.% group displayed more voids than did the 7.0 wt.% group. In addition, the 7.0 wt.% group had a smoother surface than the other groups did, and the bigger size and higher frequency of the voids could be the main reasons for the lower flexural strength.

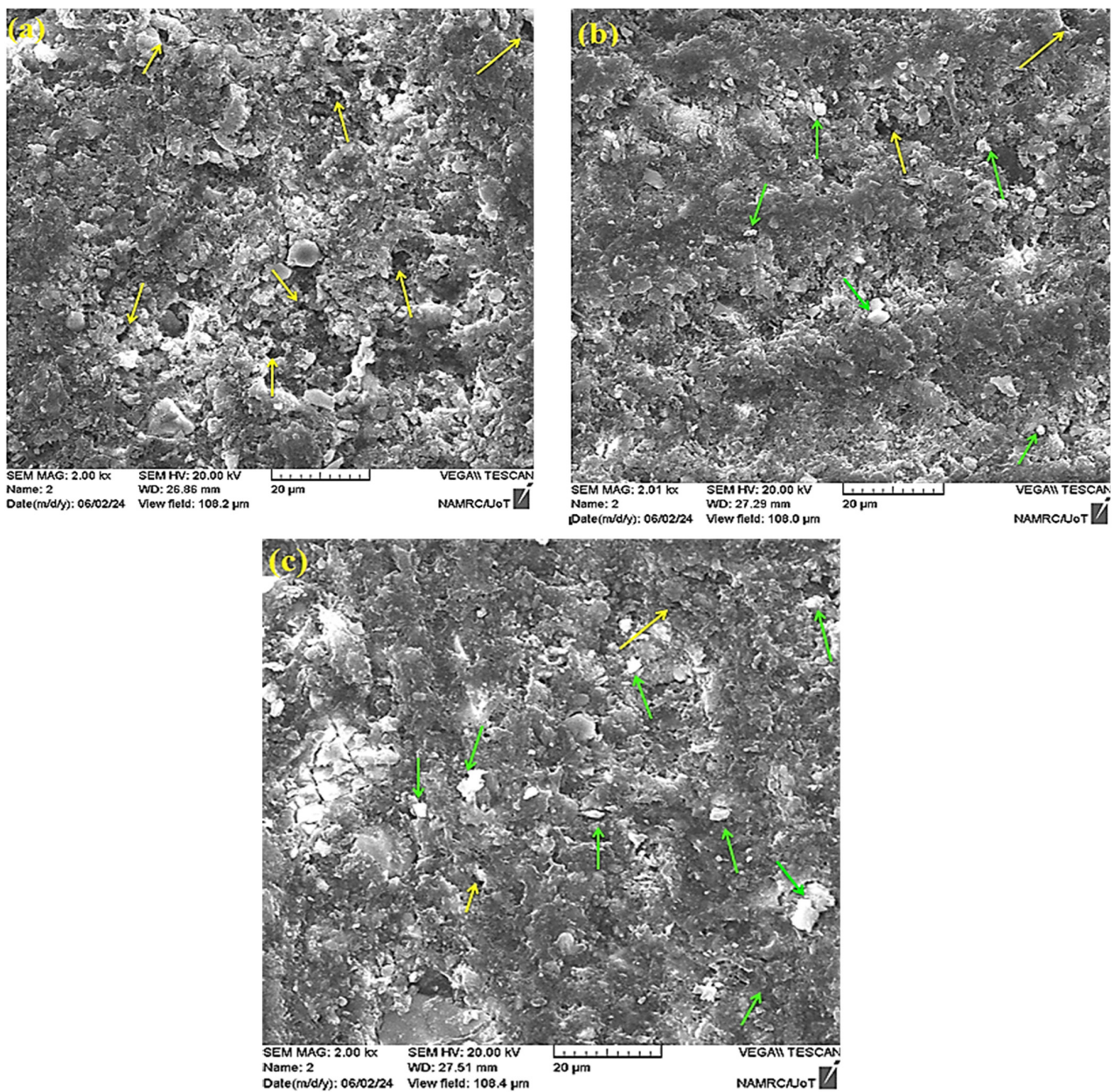


Figure 4. SEM image of 3D-printed flexural strength test samples before fracture: (a) pure acrylic resin, (b) acrylic reinforced with 5.0 wt.% GSSPs, and (c) acrylic reinforced with 7.0 wt.% GSSPs. The yellow arrows point to voids, and the green arrows point to GSSPs.

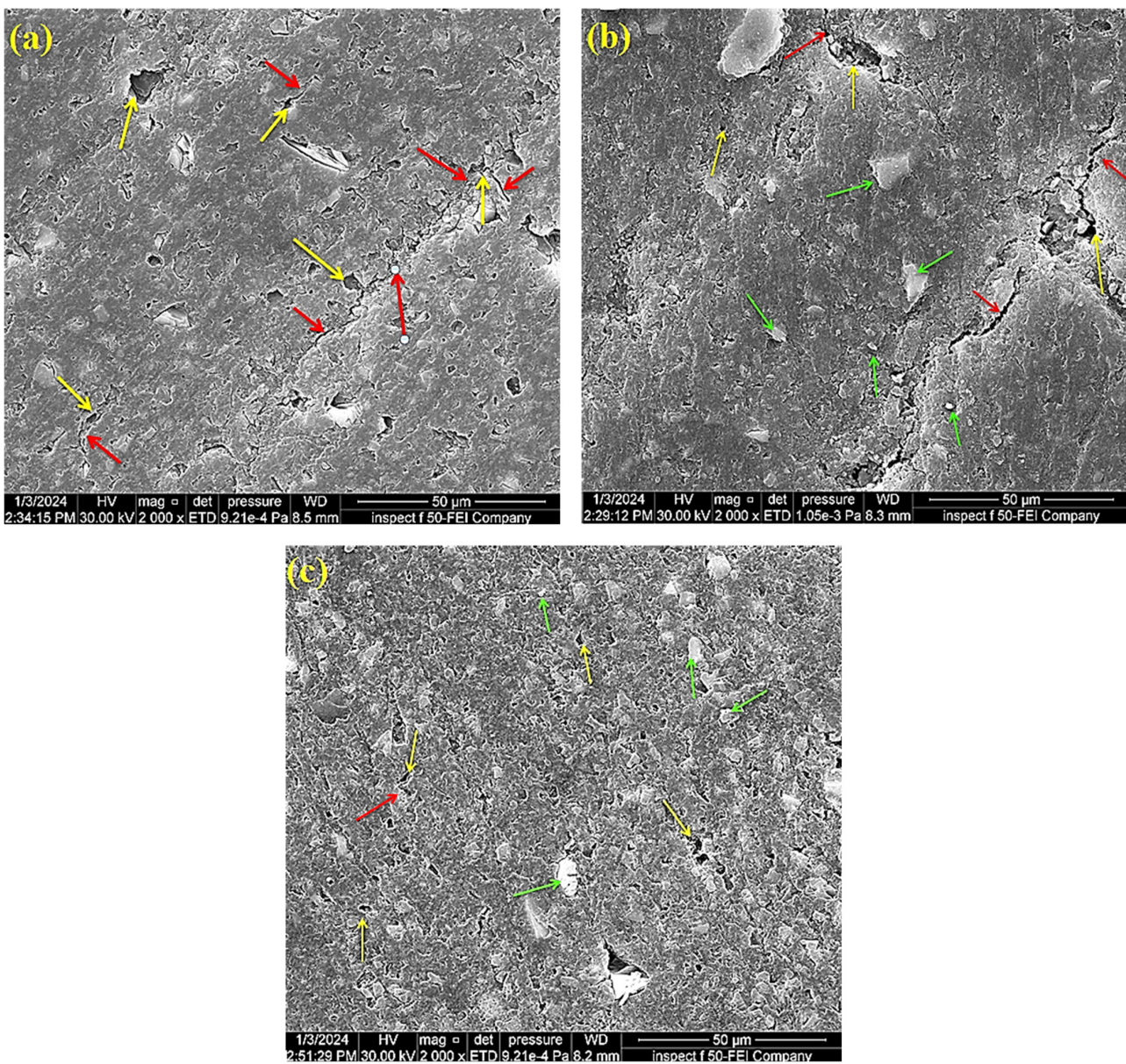


Figure 5. FE-SEM images of the fractured sites of 3D-printed flexural test samples: (a) pure acrylic resin, (b) acrylic reinforced with 5.0 wt.% GSSPs, and (c) acrylic reinforced with 7.0 wt.% GSSPs. The red arrows point to crack, the yellow arrows point to void, and the green arrows point to GSSPs.

FE-SEM images were also used to study the fracture behavior of the acrylic resin and composites. In general, the samples in all three groups exhibited brittle failure mode. However, the fracture mode in 7.0 wt.% GSSP group was more brittle than the other groups as indicated by a smoother and more compact fractured surface. Excessive stress during the flexural strength test could lead to a microcrack initiation and subsequent propagation of the cracks, resulting in a brittle fracture. The presence of voids created localized weak points and contributed to spreading the microcracks through them. Furthermore, owing to the layered deposition process in 3D printing, there could be failure due to layer delamination. However, in the fractured surfaces, no layered structure was found, indicating that the interlayer bonding was seamless and strong.

3.4. Fourier Transform Infrared (FTIR) and Degree of Conversion

Fourier transform infrared (FTIR) spectroscopy is a powerful analytical technique used to identify the functional groups in a compound and to determine its molecular structure. The FTIR spectrum of the GSSPs showed corresponding vibrations of alcohols, carboxylic acids, and esters. The absorption peaks corresponding to the vibrational modes of the functional groups in the GSSPs and 3D-printed denture base sample groups are shown in Figure 6.

The characteristic peaks of common functional groups, such as OH, C=O, NH, and CH, can be identified in the GSSP spectrum to confirm the presence of specific chemical bonds. The broad peak at approximately 3412 cm^{-1} could be due to the O–H stretching vibration. The peak observed at 2927 cm^{-1} represented the stretching vibration of the (C–H) bond in the carbohydrate ring, and strong C=O– stretching occurred at $1710\text{--}1665\text{ cm}^{-1}$. The band at 1330 cm^{-1} indicated CH₂ bending. The peaks at 1051 cm^{-1} and 1029 cm^{-1} could be due to C–O stretching and are characteristic bands of cellulose and hemicellulose from lignocellulose materials [21].

FTIR spectrum of the 3D-printed pure acrylic sample displayed two major absorption peaks: a peak attributed to the methacrylate group at approximately 1539 cm^{-1} and a peak attributed to the carbonyl ester group at approximately 1716 cm^{-1} . The peak at 3390 cm^{-1} appeared as a broad peak indicative of O–H stretching. A sharp part of the C=O peak was observed at 1716 cm^{-1} . A carbon-to-carbon C=C bond peak at 1631 cm^{-1} was also observed. The peak at 1259 cm^{-1} could be assigned to the C–O stretching mode. The peak at 2956 cm^{-1} could be due to the increased vibration of C–H bond stretching. The peaks at 1471 cm^{-1} and 1388 cm^{-1} corresponded to the –CH₂– and –CH₃ deformation vibrations, respectively. The band at 1097 cm^{-1} corresponds to the C–O bond [22].

FTIR spectra of the resin material with 5.0 wt.% GSSP highlight the presence of possible functional groups. The peaks at 1647 cm^{-1} and 3387 cm^{-1} are attributed to hydroxyl groups, OH–bending and OH–stretching, respectively. The peak at 1537 cm^{-1} corresponded to the C=C stretching vibration in the aromatic C–C bond. The peak at 1334 cm^{-1} could be attributed to the bending and stretching vibrations of CH₂. The peak at 2956 cm^{-1} was attributed to the amide I band of proteins. The band at 1095 cm^{-1} corresponded to the C–O bond in the C–OH group that allowed interaction with the fiber and was part of the azetidine ring. The absorption bands at 1728 cm^{-1} and 1469 cm^{-1} are attributed to the C=O group and C–C bending vibration, respectively [23,24].

Figure 7 shows the FTIR data for the liquid and solid control samples and the peak heights at 1635 cm^{-1} and 1716 cm^{-1} used to calculate the degree of conversion. FTIR data for the liquid and solid 5.0 wt.% GSSP samples and the peak heights at 1635 cm^{-1} and 1728 cm^{-1} used to calculate the degree of conversion are also shown. Finally, FTIR data for the liquid and solid 7.0 wt.% GSSP samples and the peak heights at 1635 cm^{-1} and 1720 cm^{-1} used to calculate the degree of conversion are shown. The degree of conversion was calculated by considering the liquid for each concentration as a baseline reference, and the mean values were 65.92, 74.70, and 73.95 for the solid (S) control/liquid (L) control, (S) 5.0 wt.% GSSPs/(L) 5.0 wt.% GSSPs and (S) 7.0 wt.% GSSPs/(L) 7.0 wt.% GSSPs, respectively. There were highly significant differences between all the groups ($p < 0.0001$), as shown in Figure 8.

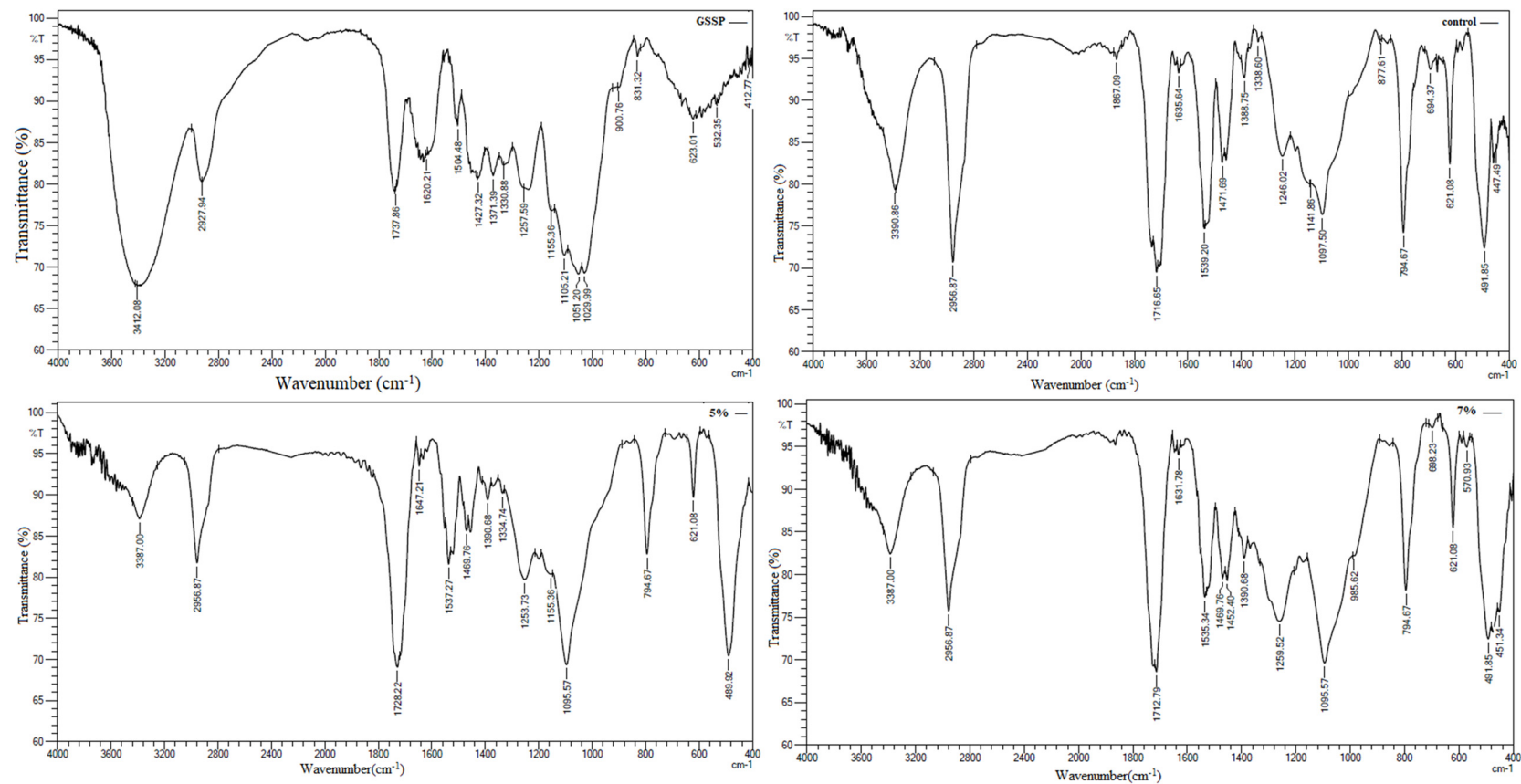


Figure 6. FTIR plots for grapefruit seed skin particles (GSSPs), control, 5.0 wt.% GSSPs, and 7.0 wt.% GSSPs groups. FTIR spectral details of the resin material with 7.0 wt.% GSSPs showed broad peak at 3387 cm^{-1} , indicative of O–H stretching. This peak could be due to the presence of hydroxyl groups in the resin or the grapefruit seed microparticles. The presence of a sharp peak at 2956 cm^{-1} indicated that C–H stretching was likely due to the presence of aliphatic hydrocarbons in the resin. The peak at 1712 cm^{-1} was attributed to carbonyl groups, which could be due to the presence of ester groups in the resin. The peak at 1631 cm^{-1} was a weak peak that could be indicative of C=C stretching. This peak could be due to the presence of alkenes in the resin or the grapefruit seed microparticles. The weak peak at 1535 cm^{-1} indicated that N–H bending could be due to the presence of amines [25].

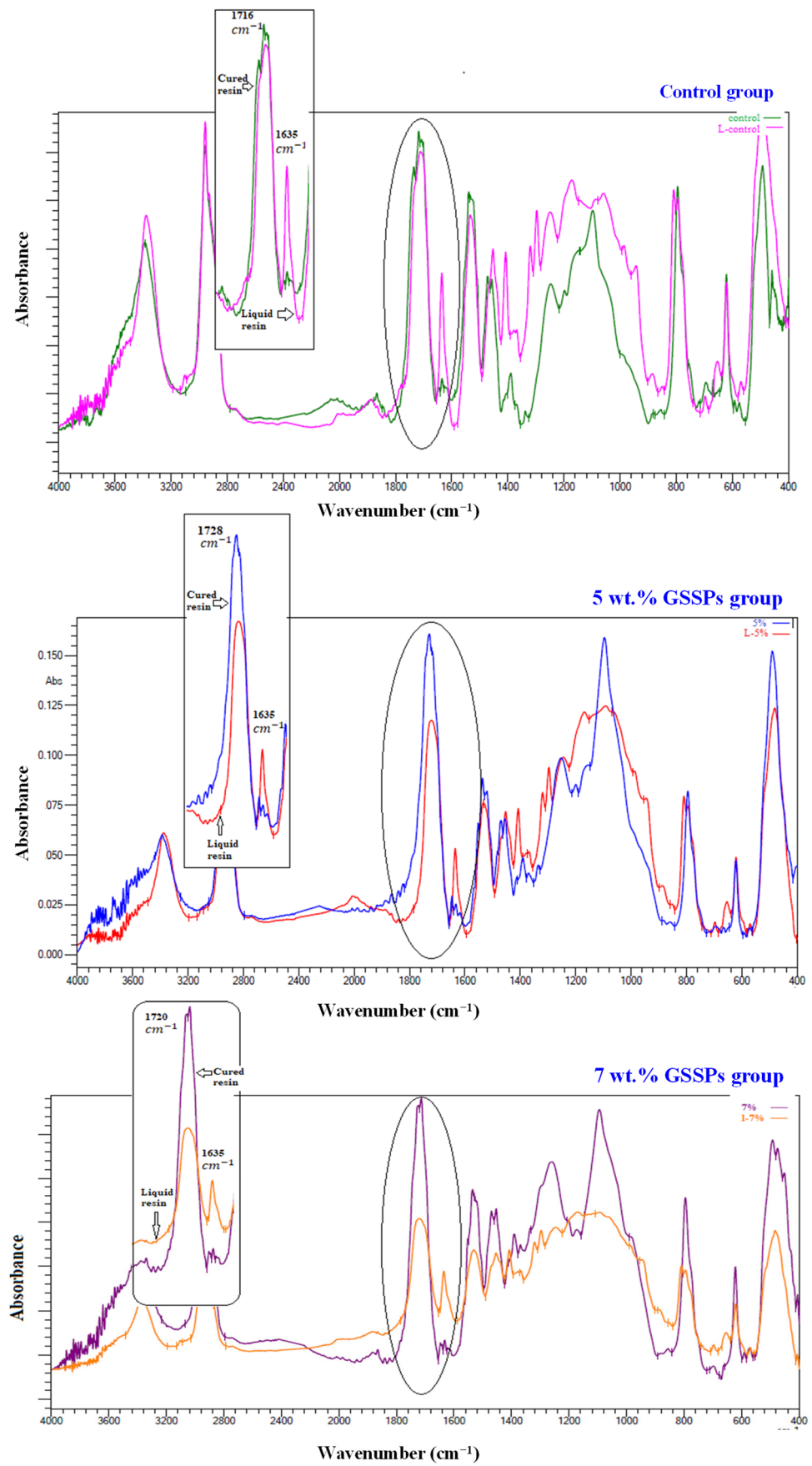


Figure 7. FTIR plots for liquid resin and corresponding solid resin to calculate degree of conversion.

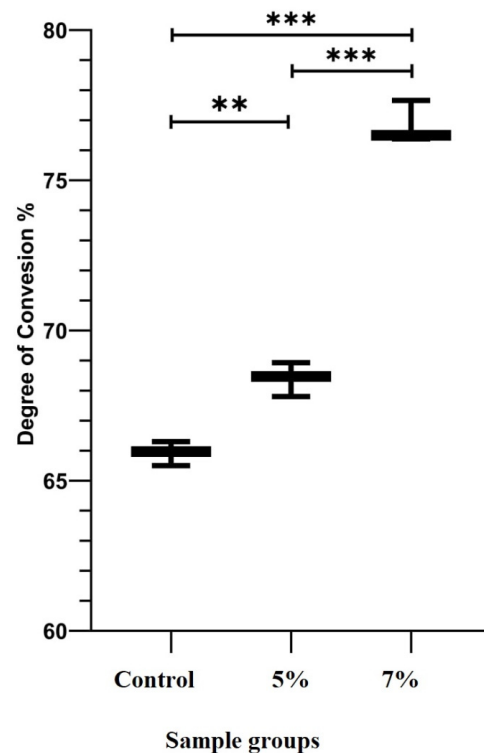


Figure 8. Boxplot for the degree of conversion with multiple comparisons labeled with ** and ***. A p value < 0.001 indicated high statistical significance (***).

4. Discussion

After the addition of GSSPs to 3D-printed denture base resin, the surface hardness, flexural strength, tensile strength, and degree of conversion significantly increased. Therefore, the null hypothesis that there would be no effect on the mechanical properties of 3D-printed denture base resin after the addition of grapefruit skin seed microparticles was rejected.

4.1. 3D Printing

The use of 3D printing in the dental industry has increased over time because of its many advantages over traditional techniques, such as fewer sessions to complete dentures, reduced dentist and technician mistakes, simple access to stored digital data, and the accuracy of the dentures produced. However, there are still some issues to address. To develop dental restorations, it is necessary to consider all factors that can withstand the forces in the oral cavity so that the dental restorations should demonstrate exceptional physical and mechanical properties [26]. Many factors may affect the development of polymers in the additive manufacturing of dentistry prostheses, such as the post-curing time, printing orientation, and filler, which may increase the viscosity of the resin and cause problems such as uneven flow, poor printability, and clogging. These fillers may settle over time, resulting in inhomogeneity, which consequently causes inferior mechanical properties in the printed objects. To achieve the best quality and printability for printable resins, careful selection of the filler type, concentration, and size is necessary [27]. Compared with SLA, DLP is preferable because it has higher accuracy, faster processing, less material consumption, and higher efficiency [28]. In this study, a layer thickness of 50 μm was used to achieve good-quality samples, which do not contain many print defects. As the thickness of the layer decreases, the strength of the printed resin increases, the dimension decreases, and better drying of the printed resin is achieved [29].

The incorporation of antimicrobial agents into denture base acrylic resin could be an alternative method for enhancing oral hygiene for people wearing dentures and for controlling oral infection. The invention of antimicrobial denture bases is considered to be

an outstanding achievement [8]. However, the physical and mechanical properties should not excessively change [30] to maintain its integrity during clinical use. Many natural materials have been added to PMMA. For example, chitosan nanoparticles extracted from the external skeleton of shellfish were added to heat-polymerized denture base resin at 5.0 wt.%, 10.0 wt.%, and 15.0 wt.% and displayed good antifungal activity against *Candida albicans* [31]. Furthermore, it did not have any effect on the tensile strength at all concentrations, but it improved the flexural strength at 5.0 wt.% [32]. Henna, also called *Lawsonia inermis*, has good antifungal properties against *Candida albicans* [8], but the flexural strength and surface hardness significantly decrease when henna powder is added to PMMA denture base material [9].

4.2. Mechanical Properties

The surface hardness is the deformation resistance of the resin, and this test was employed to evaluate the degree of resin polymerization. The degradation of the denture base impacts the longevity of the denture in the oral cavity, and when the surface hardness decreases, the denture becomes affected by brushing, which exposes it to plaque deposits and discoloration. Therefore, increased wear resistance is associated with increased surface hardness [30]. Pure resin with no addition of GSSPs has the lowest surface hardness, which could be explained by its composition and the fact that the degree of double-bond conversion in 3D-printed resin is lower than that in conventional PMMA denture material [33]. The incorporation of GSSPs into 3D-printed resin contributes to an increase in DC and stability. This increase could also be explained by the strength of the bond between the resin and GSSPs that had been proven by FTIR results. A change in the peak position and the formation of new peaks, as shown in Figure 6, indicated the presence of some chemical reaction between the GSSPs and the 3D-printed resin. For example, a sharp peak of the C=O bond was observed at 1716 cm^{-1} in the control group, which changed its position to 1728 cm^{-1} and 1712 cm^{-1} for 5.0 wt.% GSSPs and 7.0 wt.% GSSPs, respectively. Also, the presence of new peaks at 1647 cm^{-1} in the sample with 5.0 wt.% GSSPs indicated a hydroxyl group and at 1631 cm^{-1} in the sample with 7.0 wt.% GSSPs referred to a carbon-to-carbon bond. The improved DC also significantly increased the surface hardness of the experimental groups. This result disagrees with that of Nawasrah et al., who reported that the addition of henna to traditional acrylic decreased the surface hardness [34], and agrees with that of Oleiwi et al. and AlFuraiji et al., who reported that the addition of pistachio shell powder and Ti6Al4V alloy particles, respectively, to PMMA increased the surface hardness [35,36]. This result could be explained by the increased hardness and stiffness of the added particles, which increased the surface hardness of the material [37].

Cyclic denture flexing is considered to be the main cause of clinical failure. Therefore, enhancing the flexural strength of denture base materials is very important. It is defined as the maximum bending stress that a material can withstand before it yields. Denture bases are subject to both dynamic loading and static loading. Low flexural strength is clinically relevant for increased denture base fractures [38]. The results of this study revealed a statistically significant increase in flexural strength after adding 5.0 wt.% and 7.0 wt.% GSSPs compared with the control group (0.0 wt.% GSSPs). The reason for the low flexural strength in the 0.0 wt.% GSSP group might be attributed to the layer-by-layer construction process during printing, which permits the trapping of air in the resin and the formation of voids between layers, which in turn impacts the mechanical properties through propagation of microcracks. This agrees with Tian et al. who reached the conclusion that the presence of voids in glass ionomer cement plays an important role in spreading the microcracks and that the mechanical properties could be enhanced by reducing the porosity, increasing homogeneity and reinforcing glass-matrix bonding [39].

The increase in the flexural strength of the composites reinforced with the GSSPs might be attributed to the good interfacial adhesion of the matrix and the GSSPs in the reinforced 3D-printed resin, which allowed the transfer of shear stress from the GSSPs to the matrix. Furthermore, as the concentration of GSSPs increased, the interfacial contact area increased,

which led to increased flexural strength. This study agreed with that of Chander and Venkatraman [32], who reported that adding chitosan to denture base resin improved the flexural strength of the material. However, Gad et al. reported that adding henna to denture base resin had a negative effect on flexural strength [9]. This difference in results could be explained by the poor dispersion of the henna microfillers in the resin matrix.

The degree of conversion improved with increasing concentrations of GSSPs, resulting in a reduced amount of unreacted monomer and enhanced mechanical properties. This agrees with the findings of Altarazi et al., who reported that adding 0.1 wt.% TiO_2 to 3D-printed liquid resin significantly increased the degree of conversion [40]. The major mechanical property associated with denture base fracture is flexural strength, and, according to the ISO (ISO-20795-1:2013), 65 MPa is the minimum strength required for the clinical success of the denture base materials. In this study, the flexural strength of the samples in the control group was 66.36 MPa, which increased to 73.48 MPa after adding 5.0 wt.% GSSPs and 77.98 MPa with 7.0 wt.% GSSPs. This statistically significant increase in flexural strength could lead to improvements in clinical outcomes.

In this study, 3D-printed denture base resin was investigated instead of conventional acrylics with the purpose of replacing them with 3D-printed resins with enhanced mechanical properties. Dentures made of conventional heat-cured PMMA have many drawbacks, such as the large number of clinical visits required by patients to complete the denture fit for purpose. Owing to the presence of several manufacturing techniques and differences in the composition of the materials, a wide range of flexural strength values have been reported for 3D-printed denture base resins and conventional heat-cured resins [2,41]. However, heat-cured PMMA generally has greater flexural strength than 3D-printed pure resin. For example, Chhabra et al. [2] reported a greater mean flexural strength for heat-cured acrylic resin (92.01 ± 12.14 MPa) than for 3D-printed denture base resin (69.78 ± 7.54 MPa). Additionally, Al-Dwairi et al. [42] found greater flexural strength for heat-cured acrylic (92.44 ± 7.91 MPa) than for other 3D-printed resins, such as Dentona (81.33 ± 5.88 MPa), ASIGA (79.33 ± 6.07 MPa), and NextDent (74.89 ± 8.44 MPa). In contrast, the current result of the pure Dentona resin (66.36 ± 0.8339 MPa) is significantly lower. However, the 7.0 wt.% GSSPs reinforced Dentona resin produced highly encouraging results (77.98 ± 1.663 MPa).

Evaluating the success of dentures is important because the alveolar absorption process leaves irregular alveoli that make dentures subject to uneven loads [43]. In the oral cavity, dentures are subjected to many deforming loads, which may cause fracture during use [30]. It is extremely difficult to create pure tensile stress in a sample, which is the tension created by a load that works to elongate or stretch the sample. The tensile stress and tensile strain are always combined. The justification for this is that tensile loading causes a small amount of flexural stress. The elements of the stress distribution are tension, shear, and compression. Tensile tests provide useful information about the strength features of polymers [18,30]. The fillers were used to strengthen the denture base [44]. The results of the study revealed a significant increase in the tensile strength of the experimental groups. Good bonding between the 3D-printed resin matrix and the GSSPs increased the tensile strength, as demonstrated by the results. The control group had a tensile strength of 15.1 MPa, whereas after the addition of 5.0 wt.% GSSPs, the tensile strength increased to 17.81 MPa, and the highest mean value was 21.04 MPa after the addition of 7.0 wt.% GSSPs. The results of this study agree with those of Fatalla et al., who reported that the addition of polyester micro-filler particles to a light-cured denture base material (Aurora VLC) increased the tensile strength [45]. This could be explained by the ability of microparticles to fill the pores and gaps that exist within the material, which improved the degree of molecular attraction and, in turn, increased the tensile strength. In contrast, Song et al. [46] reported no effect on the tensile strength when chitosan was added to acrylic resin.

4.3. Microstructural Characteristics of the Fractured Surface

FE-SEM images revealed a uniform distribution of the GSSPs within the resin matrix, and the presence of voids in the control sample decreased after the GSSPs were added. This could be due to the adoption of an effective mixing method, where the temperature of the resin was increased to 60 °C for 30 min to decrease the viscosity, and the GSSPs were gradually added with continuous and slow mixing for 8 h at room temperature. This decrease in viscosity allowed the GSSPs to distribute without causing any particle agglomeration. After the addition of the GSSPs to the 3D-printed resin, the voids decreased, and the DC improved, which enhanced the mechanical properties of the resulting material.

4.4. Clinical Significance, Limitations, and Future Work

The focus on the development of 3D-printed denture base resins has increased over the past few years. There are encouraging results with respect to the mechanical properties in terms of surface hardness and flexural strength [26]. The addition of GSSPs to 3D-printed resin could be beneficial for improving the mechanical properties for future clinical applications.

Importantly, in this study, only one type of 3D-printed resin (Dentona) with one printing orientation of 45 degrees and a specific post-printing polymerization process were used. Therefore, further studies can be carried out with other 3D-printed resins reinforced with GSSPs, as the type of resin used could affect the current results. Although this study revealed the encouraging mechanical properties of 3D-printed denture base resin reinforced with GSSPs under dry conditions, further studies assessing the mechanical properties under accelerated aging in water, artificial saliva, and coffee, which reflect the real oral environment, are needed. Other properties of the materials, such as surface roughness, optical characteristics, and water sorption and solubility, also need to be evaluated to ensure long-term clinical stability. Finally, the antifungal resistance of the GSSP-reinforced composites against denture stomatitis will be evaluated to ensure the multi-dimensional benefits of natural seed skin particles in denture base resin.

5. Conclusions

For the first time, micro-sized grapefruit seed skin particles (GSSPs) were successfully incorporated into Dentona 3D-printed resin via a DLP printer at 5.0 wt.% and 7.0 wt.% GSSP concentrations. Within the limitations of this study, the addition of GSSPs to 3D-printed denture bases significantly increased the mechanical properties, such as surface hardness, flexural strength, and tensile strength, compared with those of pure resin. An increase in the concentration of GSSPs led to an increase in the degree of conversion. FESEM revealed a decrease in the size and number of voids as the concentration of the GSSPs increased.

Author Contributions: Conceptualization, M.M.S. and A.A.F.; methodology, M.M.S., A.A.F. and J.H.; validation, A.A.F. and J.H.; formal analysis, M.M.S., A.A.F. and J.H.; investigation, M.M.S. and A.A.F.; resources A.A.F.; data curation, M.M.S.; writing—original draft preparation, M.M.S. and A.A.F.; writing—review and editing, A.A.F. and J.H.; visualization, A.A.F. and J.H.; supervision, A.A.F. and J.H.; project administration, A.A.F.; funding acquisition, M.M.S. All authors have read and agreed to the published version of the manuscript.

Funding: This research received no external funding.

Institutional Review Board Statement: Not applicable.

Informed Consent Statement: Not applicable.

Data Availability Statement: The data presented in this study are available on request from the corresponding author.

Acknowledgments: The authors would like to acknowledge the supports from University of Baghdad.

Conflicts of Interest: The authors declare no conflicts of interest.

References

1. Polzer, I.; Schimmel, M.; Müller, F.; Biffar, R. Edentulism as part of the general health problems of elderly adults. *Int. Dent. J.* **2010**, *60*, 143–155. [[PubMed](#)]
2. Chhabra, M.; Kumar, M.N.; RaghavendraSwamy, K.N.; Thippeswamy, H.M. Flexural strength and impact strength of heat-cured acrylic and 3D printed denture base resins—A comparative in vitro study. *J. Oral Biol. Craniofacial Res.* **2022**, *12*, 1–3. [[CrossRef](#)] [[PubMed](#)]
3. Hull, C.W. Apparatus for Production of Three-Dimensional Objects by Stereolithography. U.S. Patent Application No. 638905, 8 August 1984.
4. Crump, S.S. Apparatus and Method for Creating Three-Dimensional Objects. U.S. Patent Application No. 5,121,329/1992, 9 June 1992.
5. ASTM International. *ASTM Committee F42 on Additive Manufacturing Technologies*; ASTM International: West Conshohocken, PA, USA, 2012.
6. Revilla-León, M.; Meyers, M.J.; Zandinejad, A.; Özcan, M. A review on chemical composition, mechanical properties, and manufacturing work flow of additively manufactured current polymers for interim dental restorations. *J. Esthet. Restor. Dent.* **2019**, *31*, 51–57. [[CrossRef](#)] [[PubMed](#)]
7. Yarborough, A.; Cooper, L.; Duqum, I.; Mendonça, G.; McGraw, K.; Stoner, L. Evidence regarding the treatment of denture stomatitis. *J. Prosthodont.* **2016**, *25*, 288–301. [[CrossRef](#)]
8. Nawasrah, A.; AlNimr, A.; Ali, A.A. Antifungal effect of henna against *Candida albicans* adhered to acrylic resin as a possible method for prevention of denture stomatitis. *Int. J. Environ. Res. Public Health* **2016**, *13*, 520. [[CrossRef](#)]
9. Gad, M.; Rahoma, A.; Nawasra, A.; Ammar, M. Influence of henna addition on the flexural strength of acrylic denture base material: An in vitro study. *Al-Azhar Dent. J. Girls.* **2018**, *5*, 277–283. [[CrossRef](#)]
10. Ikono, R.; Vibriani, A.; Wibowo, I.; Saputro, K.E.; Muliawan, W.; Bachtiar, B.M.; Mardiyati, E.; Bachtiar, E.W.; Rochman, N.T.; Kagami, H.; et al. Nanochitosan antimicrobial activity against *Streptococcus mutans* and *Candida albicans* dual-species biofilms. *BMC Res. Notes* **2019**, *12*, 383. [[CrossRef](#)] [[PubMed](#)]
11. Al-Shammari, S.S.; Abdul-Ameer, F.M.; Bairam, L.R.; Al-Salihi, Z. The influence of lemongrass essential oil addition into heat cured acrylic resin against *Candida albicans* adhesion. *J. Baghdad Coll. Dent.* **2023**, *35*, 67–75. [[CrossRef](#)]
12. Noori, Z.S.; Al-Khafaji, A.M.; Dabaghi, F. Effect of tea tree oil on candida adherence and surface roughness of heat cure acrylic resin. *J. Baghdad Coll. Dent.* **2023**, *35*, 46–54. [[CrossRef](#)]
13. Kang, S.T.; Son, H.K.; Lee, H.J.; Choi, J.S.; Choi, Y.I.; Lee, J.J. Effects of grapefruit seed extract on oxidative stability and quality properties of cured chicken breast. *Korean J. Food Sci. Anim. Resour.* **2017**, *37*, 429. [[CrossRef](#)] [[PubMed](#)]
14. Bahrin, L.G.; Apostu, M.O.; Birsă, L.M.; Stefan, M. The antibacterial properties of sulfur containing flavonoids. *Bioorg Med. Chem. Lett.* **2014**, *24*, 2315–2318. [[CrossRef](#)]
15. Bartoloni, J.A.; Murchison, D.F.; Wofford, D.T.; Sarkar, N.K. Degree of conversion in denture base materials for varied polymerization techniques 1. *J. Oral Rehabil.* **2000**, *27*, 488–493. [[CrossRef](#)]
16. Farooq Anwar, F.A.; Rehana Naseer, R.N.; Bhangar, M.I.; Samia Ashraf, S.A.; Talpur, F.N.; Aladedunye, F.A. Physico-chemical characteristics of citrus seeds and seed oils from Pakistan. *J. Am. Oil Chem. Soc.* **2008**, *85*, 321–330. [[CrossRef](#)]
17. Dunlap, R.A.; Small, D.A.; MacKay, G.R.; O'Brien, J.W.; Dahn, J.R.; Cheng, Z.H. Materials preparation by ball milling. *Can. J. Phys.* **2000**, *78*, 211–229. [[CrossRef](#)]
18. Al-Sammraie, M.F.; Fatalla, A.A.; Atarchi, Z.R. Assessment of the correlation between the tensile and diametrical compression strengths of 3D-printed denture base resin reinforced with ZrO₂ nanoparticles. *J. Baghdad Coll. Dent.* **2024**, *36*, 44–53. [[CrossRef](#)]
19. Mudhaffer, S.; Althagafi, R.; Haider, J.; Satterthwaite, J.; Silikas, N. Effects of printing orientation and artificial ageing on martens hardness and indentation modulus of 3D printed restorative resin materials. *Dent. Mater.* **2024**, *40*, 1003–1014. [[CrossRef](#)] [[PubMed](#)]
20. Fareed Al-Sammraie, M.; Fatalla, A.A. The effect of ZrO₂ NPs addition on denture adaptation and diametral compressive strength of 3D printed denture base resin. *Nanomed. Res. J.* **2023**, *8*, 345–355.
21. Kanmani, P.; Dhivya, E.; Aravind, J.; Kumaresan, K. Extraction and analysis of pectin from citrus peels: Augmenting the yield from Citrus limon using statistical experimental design. *Iran. J. Energy Environ.* **2014**, *5*, 303–312. [[CrossRef](#)]
22. Yong, Q.; Liang, C. Synthesis of an aqueous self-matting acrylic resin with low gloss and high transparency via controlling surface morphology. *Polymers* **2019**, *11*, 322. [[CrossRef](#)]
23. Chua, S.C.; Chong, F.K.; Ul Mustafa, M.R.; Mohamed Kutty, S.R.; Sujarwo, W.; Abdul Malek, M.; Show, P.L.; Ho, Y.C. Microwave radiation-induced grafting of 2-methacryloyloxyethyl trimethyl ammonium chloride onto lentil extract (LE-g-DMC) as an emerging high-performance plant-based grafted coagulant. *Sci. Rep.* **2020**, *10*, 3959. [[CrossRef](#)]
24. Pandian, S.R.K.; Deepak, V.; Kalishwaralal, K.; Gurunathan, S. Biologically synthesized fluorescent CdS NPs encapsulated by PHB. *Enzyme Microb. Technol.* **2011**, *48*, 319–325. [[CrossRef](#)]
25. Sitheeque, M.A.M.; Panagoda, G.J.; Yau, J.; Amarakoon, A.M.T.; Udagama, U.R.N.; Samaranyake, L.P. Antifungal activity of black tea polyphenols (catechins and theaflavins) against *Candida* species. *Chemotherapy* **2009**, *55*, 189–196. [[CrossRef](#)]
26. Gad, M.M.; Al-Harbi, F.A.; Akhtar, S.; Fouda, S.M. 3D-printable denture base resin containing SiO₂ nanoparticles: An in vitro analysis of mechanical and surface properties. *J. Prosthodont.* **2022**, *31*, 784–790. [[CrossRef](#)] [[PubMed](#)]

27. Qaisar, A.; Jatala, U.W.; Fareed, M.A.; Yazdanie, N. Measurement of residual monomer in autopolymerized acrylic resins by high pressure liquid chromatography. *Biomedica* **2017**, *33*, 211.
28. Kessler, A.; Hickel, R.; Reymus, M. 3D printing in dentistry-state of the art. *Oper. Dent.* **2020**, *45*, 30–40. [[CrossRef](#)] [[PubMed](#)]
29. Alshamrani, A.A.; Raju, R.; Ellakwa, A. Effect of printing layer thickness and postprinting conditions on the flexural strength and hardness of a 3D-printed resin. *Biomed. Res. Int.* **2022**, *2022*, 8353137. [[CrossRef](#)] [[PubMed](#)]
30. Shen, C.; Rawls, H.R.; Esquivel-Upshaw, J.F. *Phillips' Science of Dental Materials E-Book: Phillips' Science of Dental Materials E-Book*; Elsevier Health Sciences: Amsterdam, The Netherlands, 2021.
31. Gondim, B.L.C.; Castellano, L.R.C.; de Castro, R.D.; Machado, G.; Carlo, H.L.; Valença, A.M.G.; de Carvalho, F.G. Effect of chitosan nanoparticles on the inhibition of *Candida* spp. *biofilm* on denture base surface. *Arch. Oral Biol.* **2018**, *94*, 99–107. [[CrossRef](#)]
32. Chander, N.G.; Venkatraman, J. Mechanical properties and surface roughness of chitosan reinforced heat polymerized denture base resin. *J. Prosthodont. Res.* **2022**, *66*, 101–108. [[CrossRef](#)]
33. Alifui-Segbaya, F.; Bowman, J.; White, A.R.; George, R.; Fidan, I. Characterization of the double bond conversion of acrylic resins for 3D printing of dental prostheses. *Compend. Contin. Educ. Dent.* **2019**, *40*, 7–11.
34. Nawasrah, A.; Gad, M.; El Zayat, M. Effect of henna addition on the surface roughness and hardness of polymethylmethacrylate denture base material: An in-vitro study. *J. Contemp. Dent. Pr.* **2018**, *19*, 732–738. [[CrossRef](#)]
35. Oleiwi, J.; Hamad, Q.A.; Kadhim, N.N. Study compression, hardness and density properties of PMMA reinforced by natural powder used in denture base applications. *Eng. Technol. J.* **2019**, *37*, 522–527. [[CrossRef](#)]
36. AlFuraiji, N.H.; Altaie, S.F.; Qasim, S.S. Evaluating the influence of Ti₆Al₄V alloy particles on mechanical properties of heat-cured PMMA. *J. Baghdad Coll. Dent.* **2024**, *36*, 44–53. [[CrossRef](#)]
37. Hamad, Q.A. Fabrication and Characterization of Denture Base Material by Hybrid Composites from Self Cured PMMA Resin. Ph.D. Thesis, University of Technology, Materials Engineering Department, Hong Kong, China, 2015.
38. Prpić, V.; Schauerperl, Z.; Čatić, A.; Dulčić, N.; Čimić, S. Comparison of mechanical properties of 3D-printed, CAD/CAM, and conventional denture base materials. *J. Prosthodont.* **2020**, *29*, 524–528. [[CrossRef](#)]
39. Tian, K.V.; Nagy, P.M.; Chass, G.A.; Fejerdy, P.; Nicholson, J.W.; Csizmadia, I.G.; Dobó-Nagy, C. Qualitative assessment of microstructure and Hertzian indentation failure in biocompatible glass ionomer cements. *J. Mater. Sci. Mater. Med.* **2012**, *23*, 677–685. [[CrossRef](#)] [[PubMed](#)]
40. Altarazi, A.; Haider, J.; Alhotan, A.; Silikas, N.; Devlin, H. 3D printed denture base material: The effect of incorporating TiO₂ nanoparticles and artificial ageing on the physical and mechanical properties. *Dent. Mater.* **2023**, *39*, 1122–1136. [[CrossRef](#)] [[PubMed](#)]
41. Lourinho, C.; Salgado, H.; Correia, A.; Fonseca, P. Mechanical properties of polymethyl methacrylate as denture base material: Heat-polymerized vs. 3D-printed—Systematic review and meta-analysis of in vitro studies. *Biomedicines* **2022**, *10*, 2565. [[CrossRef](#)] [[PubMed](#)]
42. Al-Dwairi, Z.N.; Al Haj Ebrahim, A.A.; Baba, N.Z. A comparison of the surface and mechanical properties of 3D printable denture-base resin material and conventional polymethylmethacrylate (PMMA). *J. Prosthodont.* **2023**, *32*, 40–48. [[CrossRef](#)]
43. Diaz-Arnold, A.M.; Vargas, M.A.; Shaull, K.L.; Laffoon, J.E.; Qian, F. Flexural and fatigue strengths of denture base resin. *J. Prosthet. Dent.* **2008**, *100*, 47–51. [[CrossRef](#)]
44. Ihab, N.S.; Hassanen, K.A.; Ali, N.A. Assessment of zirconium oxide nano-fillers incorporation and silanation on impact, tensile strength and color alteration of heat polymerized acrylic resin. *J. Bagh Coll. Dent.* **2012**, *24*, 36–42.
45. Fatalla, A.A. The effect of polyester micro-particles powder addition on some mechanical properties of light cured denture base material. *J. Int. Dent. Med. Res.* **2018**, *11*, 495–502.
46. Song, R.; Zhong, Z.; Lin, L. Evaluation of chitosan quaternary ammonium salt-modified resin denture base material. *Int. J. Biol. Macromol.* **2016**, *85*, 102–110. [[CrossRef](#)] [[PubMed](#)]

Disclaimer/Publisher's Note: The statements, opinions and data contained in all publications are solely those of the individual author(s) and contributor(s) and not of MDPI and/or the editor(s). MDPI and/or the editor(s) disclaim responsibility for any injury to people or property resulting from any ideas, methods, instructions or products referred to in the content.